JOURNAL OF SOLID STATE CHEMISTRY 73, 151–159 (1988)

The Luminescence of the Sb^{3+} Ion in $Ln(PO_3)_3$ (Ln = Sc, Lu, Y, Gd, La)

E. W. J. L. OOMEN,* R. C. M. PEETERS, W. M. A. SMIT, AND G. BLASSE

Physical Laboratory, State University of Utrecht, P.O. Box 80.000, 3508 TA Utrecht, The Netherlands

Received May 21, 1987

The efficient luminescence of the $5s^2$ ion Sb^{3+} in $Ln(PO_3)_3$ (Ln = Sc, Lu, Y, Gd, La) is reported. The compounds $Ln(PO_3)_3$ (Ln = Sc, Lu, Y, Gd) adopt the $Yb(PO_3)_3$ structure in which four slightly different octahedral sites are available for the trivalent cation, while $La(PO_3)_3$ has the $Nd(PO_3)_3$ structure in which only one position with eight coordination is available for the cation. The emission and excitation spectra of $Ln(PO_3)_3$–Sb^{3+} (Ln = Sc, Lu, Gd) show broad bands, caused by the strongly overlapping bands of the four Sb^{3+} centers. The spectra and decay time measurements show that the differences in luminescence characteristics between the four Sb^{3+} centers become more apparent with decreasing radius of the host lattice cation. The luminescence properties of $Y(PO_3)_3$–Sb^{3+} are rather complex and lead to the conclusion that the relaxed excited state of some of the Sb^{3+} centers is distorted by a Jahn–Teller effect. The luminescence of $La(PO_3)_3$–Sb^{3+} originates from one Sb^{3+} center and can be described by usual models

1. Introduction

It is well known that the luminescence properties of s^2 ions depend strongly on the host lattice (*1–3*). In order to get more insight into the lattice dependence of the luminescence of trivalent s^2 ions, we perform a systematic study on the luminescence of the Sb^{3+} ion in inorganic host lattices. Recently, we reported on the luminescence of Sb^{3+} in $LnBO_3$ (Ln = Sc, Lu, Y, Gd, La) (*4*) and $LnPO_4$ (Ln = Sc, Lu, Y) (*5, 6*). The orthophosphate $LnPO_4$–Sb^{3+} system was of special interest, since the excited states of the Sb^{3+} ion in this lattice are, both in excitation and emission, clearly distorted by the Jahn–Teller effect. In this paper we report on the luminescence of Sb^{3+} in the metaphosphates $Ln(PO_3)_3$ (Ln = Sc, Lu, Y, Gd, La).

The structures of these metaphosphates were determined by Melnikov *et al.* (*7*). $La(PO_3)_3$ has the $Nd(PO_3)_3$ structure, which has been described by Hong (*8*). In this structure one crystallographic site is available for the trivalent cation which is surrounded by eight oxygen ions forming LnO_8 dodecahedra. The other metaphosphates adopt the $Yb(PO_3)_3$ structure (*7, 9*), which has also been described by Hong (*10*). In this structure four slightly different crystallographic sites are available for the trivalent cation. In all these sites the cations are coordinated by six oxygen atoms to form slightly distorted octahedra which are isolated from each other. The cation–oxygen

* To whom correspondence should be addressed.

0022-4596/88 $3.00

distances are slightly different from site to site. In the case of $Yb(PO_3)_3$ two of these sites have inversion symmetry, while the symmetry of the other two sites is low. Preliminary investigations on the luminescence of Eu^{3+} in $Sc(PO_3)_3$ and $Gd(PO_3)_3$ reveal that also in these metaphosphates there are two sites with inversion symmetry and two sites without inversion symmetry (*11*).

2. Experimental

2.1. Sample Preparation

Starting materials were Sc_2O_3, Y_2O_3, Gd_2O_3 (all Highways International, 99.999%), Lu_2O_3 (Highways International, 99.99%), La_2O_3 (Highways International, 99.997%), Sb_2O_3, and $(NH_4)_2HPO_4$ (both Merck, p.a.).

Samples $Ln(PO_3)_3$–Sb^{3+} (*Ln* = Sc, Lu, Y, Gd, La) were prepared by mixing stoichiometric quantities of Ln_2O_3, Sb_2O_3, and $(NH_4)_2HPO_4$ (15 mole%, excess), and firing this mixture in air for 1 hr at 400°C, 1 hr at 700°C, and 1 hr at 1000°C. The obtained composition is reground and fired for another hour at 1000°C.

For reasons which will become clear later, one sample of $Y(PO_3)_3$–Sb^{3+} was prepared starting from $Y_{2-x}Sb_xO_3$. This mixed oxide was obtained by dissolving Y_2O_3 and Sb_2O_3 in hydrochloric acid (Baker, 36%, A.R.) and precipitating the metal ions as hydroxides by adding ammonia (Merck, 25%, p.a.). The precipitate was then washed, dried, and fired in air for 3 hr at 500°C. The obtained oxide was mixed with $(NH_4)_2HPO_4$ and fired as described above.

All samples were checked by X-ray diffraction using Cu$K\alpha$ radiation. Samples were prepared with a varying starting amount of Sb_2O_3. Some of these samples were analyzed by atomic absorption spectroscopy to determine the actually built-in amount of Sb. As shown in Table I, this amount varies strongly, most likely depending on the host lattice and the starting amount of Sb_2O_3.

TABLE I

ANTIMONY CONTENT (MOLE %) OF SEVERAL METAPHOSPHATE SAMPLES

Composition	Weighted-in amount Sb	Built-in amount Sb
$Sc(PO_3)_3$–Sb^{3+}	5	0.3
$Lu(PO_3)_3$–Sb^{3+}	2	0.7
$Y(PO_3)_3$–Sb^{3+}	3	3.0
	10	5.2
$Gd(PO_3)_3$–Sb^{3+}	5	1.4
$La(PO_3)_3$–Sb^{3+}	1	0.3

2.2. Optical Instrumentation

The instrumentation is the same as described in Ref. (*6*). Quantum efficiencies at 300 K were estimated by comparing the samples with commercial Sb^{3+}-activated calciumhalophosphate.

3. Results and Discussion

3.1. $Sc(PO_3)_3$–Sb^{3+}, $Lu(PO_3)_3$–Sb^{3+}, and $Gd(PO_3)_3$–Sb^{3+}

Spectra. All samples show a bluish luminescence under UV excitation with a quantum efficiency of about 70% at 300 K. Figure 1 shows the excitation spectrum of $Sc(PO_3)_3$–Sb^{3+} at different temperatures. At low temperature the excitation band exhibits a doublet structure. At higher temperatures this doublet structure vanishes. The emission spectrum of $Sc(PO_3)_3$–Sb^{3+} at 5 K is given in Fig. 2 for three different excitation wavelengths. At this temperature the position of the emission band is slightly dependent on the excitation wavelength. This dependence vanishes at higher temperatures. The broad emission band is then found at 24,700 cm^{-1}.

The excitation spectra of $Lu(PO_3)_3$–Sb^{3+} and $Gd(PO_3)_3$–Sb^{3+} consist, even at 5 K, of one broad band. The excitation maxima are

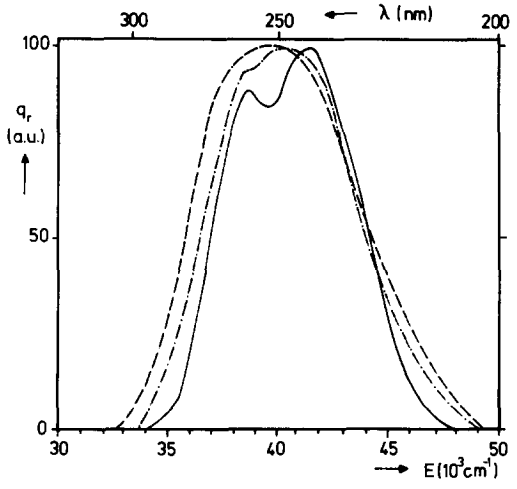

FIG. 1. Excitation spectrum of the emission of $Sc(PO_3)_3$–Sb^{3+} for T = 5 K (—), 180 K (-·-·-), and 280 K (---). The emission wavelength is selected using a cut-off filter ($\lambda_{em} > 360$ nm) and a band-pass filter ($380 < \lambda_{em} < 420$ nm). q_r represents the relative quantum output in arbitrary units. All spectra are normalized.

found at 40,500 cm^{-1} for $Lu(PO_3)_3$–Sb^{3+} and 41,000 cm^{-1} for $Gd(PO_3)_3$–Sb^{3+}. For all excitation wavelengths (even at 5 K), the emission of both compositions consists of one broad band. The emission maxima are found at 23,500 cm^{-1} ($Lu(PO_3)_3$–Sb^{3+}) and 22,000 cm^{-1} ($Gd(PO_3)_3$–Sb^{3+}).

For all compositions the excitation and emission bands broaden at increasing temperature. No temperature quenching is observed up to room temperature (RT). The luminescence properties of the samples show no dependence on the Sb concentration. Furthermore, we note that no energy transfer from Sb^{3+} to Gd^{3+} ions or reverse is observed in $Gd(PO_3)_3$–Sb^{3+} due to the lack of spectral overlap between the emission and excitation bands of these ions.

For all three compositions the excitation band is ascribed to the $^1S_0 \rightarrow {}^3P_1$ transition. The emission band is ascribed to the $^3P_1 \rightarrow {}^1S_0$ transition and at low temperatures to the $^3P_0 \rightarrow {}^1S_0$ transition, as indicated by decay time measurements (see below). The positions of these bands are in good agreement with those of the corresponding bands for Sb^{3+} in other oxidic compositions (*4*, *6*, *12*).

In all three compositions four slightly different sites for the Sb^{3+} ion are available. The low temperature structure in the excitation spectrum of $Sc(PO_3)_3$–Sb^{3+} is ascribed to the occurrence of Sb^{3+} ions on different sites (see Fig. 1). This is in line with the slight changes in the position of the emission band at different excitation wavelengths (Fig. 2). At higher temperature the emission and excitation bands broaden and these features vanish.

Since even at low temperature only one broad excitation and emission band is observed for $Lu(PO_3)_3$–Sb^{3+} and $Gd(PO_3)_3$–Sb^{3+}, the influence of the different sites on the luminescence properties of the Sb^{3+} ion is obviously smaller than in the case of $Sc(PO_3)_3$–Sb^{3+}. However, some evidence that also in these compositions the luminescence originates from Sb^{3+} ions on different sites results from the band widths which are broader than usual for Sb^{3+} luminescence from a single site. The full width at half maximum (FWHM) of the excitation band of Sb^{3+} in $La(PO_3)_3$, in which only one crystallographic site is available, amounts to 5000 cm^{-1} at RT. The excitation bands

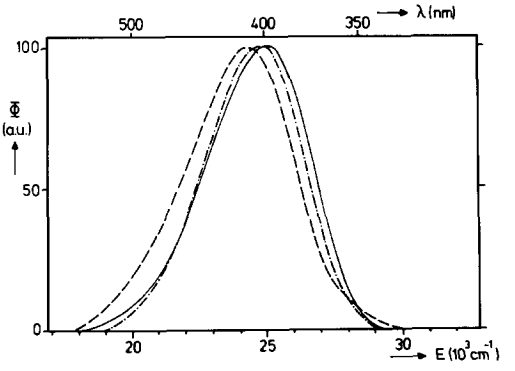

FIG. 2. Emission spectrum of $Sc(PO_3)_3$–Sb^{3+} at T = 5 K for excitation wavelength 245 nm (—), 260 nm (-·-·-), and 280 nm (---). Φ represents the radiant power per constant energy interval in arbitrary units. All spectra are normalized.

TABLE II

SPECTRAL DATA AT RT OF Sb^{3+} IN $Ln(PO_3)_3$ (Ln = Sc, Lu, Gd)

Composition	Excitation maximum	Emission maximum	FWHM of excitation band	Stokes shift	Radius host[a] lattice cation
$Sc(PO_3)_3$–Sb^{3+}	40,000	24,700	7400	15,300	0.745
$Lu(PO_3)_3$–Sb^{3+}	40,500	23,500	6100	17,000	0.861
$Gd(PO_3)_3$–Sb^{3+}	41,000	22,000	5900	19,000	0.938

Note. All values in cm^{-1}. Additionally, the radius of the host lattice cation is given (Å). See also text.

[a] Ref. (*13*).

for Sb^{3+} in other oxidic lattices, e.g., $LnBO_3$–Sb^{3+} (Ln = Sc, Lu, La) (*4*) and $LnPO_4$–Sb^{3+} (Ln = Sc, Lu, Y) (*6*), are even narrower (at RT). For $Gd(PO_3)_3$–Sb^{3+} and $Lu(PO_3)_3$–Sb^{3+} the FWHM values at RT amount to 5900 and 6100 cm^{-1}, respectively. For $Sc(PO_3)_3$–Sb^{3+} it even amounts to 7400 cm^{-1} (at RT).

The decreasing FWHM values (see Table II) in going from $Sc(PO_3)_3$–Sb^{3+} to $Gd(PO_3)_3$–Sb^{3+} suggest that the differences between the four possible Sb^{3+} sites decrease with increasing radius of the host lattice cation.

It should be kept in mind that the band positions in Table II represent the observed maxima at RT, which result from the superimposed contributions of the Sb^{3+} ions at the four different sites. The same holds for the Stokes shift, which is taken as the energy difference between the excitation and emission maxima of the $^1S_0 \rightarrow {}^3P_1$ transitions. Inspection of Table II reveals that the Stokes shift increases for increasing values of the radius of the host lattice cation. This is usually observed for dopant Sb^{3+} ions (*4, 6, 14, 15*) or other s^2 ions (for instance, Bi^{3+} (*3, 16*)) and has been ascribed to the preference of the s^2 ion for an asymmetric coordination (*17, 18*).

Decay time measurements. For all compositions the observed decay curves were not purely one-exponential. This stems from the fact that the observed curves are superpositions of four individual decay curves arising from each of the four Sb^{3+} centers. A four-exponential fitting procedure, however, yielded physically unrealistic values. As mentioned already under Introduction, there is evidence that the two sites with inversion symmetry are very similar, while the same holds for the other two sites (*10, 11*). Therefore, a two-exponential fitting procedure seems more appropriate and leads indeed to acceptable parameter values for $Sc(PO_3)_3$–Sb^{3+} and $Lu(PO_3)_3$–Sb^{3+}.

It turned out that for $Gd(PO_3)_3$–Sb^{3+} the best-fitting result could be obtained from a one-exponential fit indicating that the differences between the two pairs of Sb^{3+} centra in $Gd(PO_3)_3$ are too small to cause a well-observable difference in the decay times. This runs parallel with the consideration of the spectra given above.

The decay times as a function of temperature were fitted to the well-known three-level scheme (*19, 20*) resulting in acceptable fits for $Sc(PO_3)_3$–Sb^{3+} and $Lu(PO_3)_3$–Sb^{3+} (two-exponential decay; see Fig. 3) and for $Gd(PO_3)_3$–Sb^{3+} (one-exponential decay). The obtained values for the fitting parameters, τ_0, the decay time of the forbidden $^3P_0 \rightarrow {}^1S_0$ transition, τ_1, the decay time of the spin-orbit allowed $^3P_1 \rightarrow {}^1S_0$ transition, and ΔE, the energy difference between the $^3P_1$ and $^3P_0$ relaxed excited states are shown in Table III.

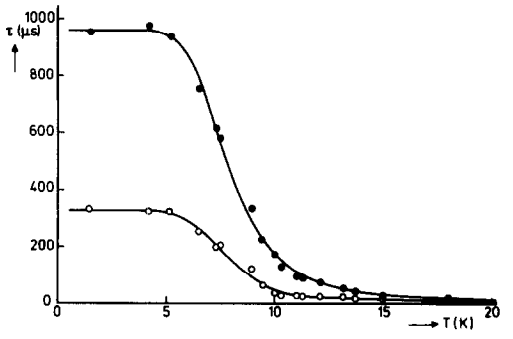

FIG. 3. Decay times versus temperature for the two pairs of Sb^{3+} centra in $Lu(PO_3)_3$. Drawn lines represent the best fits to a three-level scheme. See also text.

For s^2 ions it is generally found that ΔE decreases for increasing values of the Stokes shift (*4, 14, 15, 21*). This has been explained in terms of quenching of the spin-orbit interaction by the Jahn–Teller effect (*22*). A comparison of Tables II and III reveals that this trend is also observed for $Ln(PO_3)_3$–Sb^{3+} (Ln = Sc, Lu, Gd). This implies that a Jahn–Teller effect is acting on the excited state of the Sb^{3+} ions, although this is not observable in the spectra. The emission spectra show only one band, and a doublet structure in the excitation spectra is only found at low temperatures for $Sc(PO_3)_3$–Sb^{3+}. Because the Jahn–Teller splitting of the $^1S_0 \rightarrow {}^3P_1$ excitation band is expected to increase at increasing temperature, and because no structure is observed in the excitation bands of $Lu(PO_3)_3$–Sb^{3+} and $Gd(PO_3)_3$–Sb^{3+}, we ascribe the observed doublet shape to the influence of the different sites and not to the Jahn–Teller effect.

3.2. $Y(PO_3)_3$–Sb^{3+}

Spectra. The samples showed a bright bluish luminescence under UV excitation with a quantum efficiency of about 70% (at 300 K). The luminescence properties of $Y(PO_3)_3$–Sb^{3+} are more complex than those of $Ln(PO_3)_3$–Sb^{3+} (Ln = Sc, Lu, Gd). The emission spectra of $Y(PO_3)_3$–Sb^{3+} are shown in Fig. 4 for excitation wavelengths 245 and 260 nm. At 6 K both spectra consist of one band with its maximum around 410 nm (24,400 cm^{-1}). For higher temperatures (20 K < T < 160 K) the emission consists of two bands with maxima at about 415 nm (24,000 cm^{-1}) and 500 nm (20,000 cm^{-1}), the latter band being preferably excited at 260 nm. At still higher temperatures (T > 160 K) the emission consists of a very broad asymmetric band with its maximum around 450 nm (22,200 cm^{-1}). Up to room temperature no temperature quenching is observed.

Figure 5 shows the excitation spectra of $Y(PO_3)_3$–Sb^{3+} for emission wavelengths 400 and 500 nm. For emission wavelength 400 nm, the excitation at 5.5 K consists of a broad band with its maximum between 250

TABLE III

DECAY TIME PARAMETER VALUES OF Sb^{3+} IN $Ln(PO_3)_3$ (Ln = Sc, Lu, Gd) OBTAINED BY FITTING THE DECAY TIMES AS A FUNCTION OF TEMPERATURE TO A THREE-LEVEL SCHEME

Composition	τ_0 (μs)	τ_1 (μs)	ΔE (cm^{-1})	τ_0' (μs)	τ_1' (μs)	$\Delta E'$ (cm^{-1})
$Sc(PO_3)_3$–Sb^{3+} (2 exp)	720 ± 20	0.7 ± 0.2	45 ± 2	320 ± 20	0.6 ± 0.4	39 ± 5
$Lu(PO_3)_3$–Sb^{3+} (2 exp)	960 ± 20	0.8 ± 0.2	39 ± 2	340 ± 20	0.2 ± 0.1	41 ± 4
$Y(PO_3)_3$–Sb^{3+} (2 exp)	1040 ± 40	4 ± 3	30 ± 5	400 ± 30	7 ± 5	17 ± 4
$Y(PO_3)_3$–Sb^{3+} (1 exp)	920 ± 20	2 ± 2	37 ± 4			
$Gd(PO_3)_3$–Sb^{3+} (1 exp)	1260 ± 20	2.0 ± 0.5	32 ± 1			

Note. The decay times are obtained by fitting the experimental decay curves to a one-exponential (1 exp) or to a two-exponential fit (2 exp). See also text.

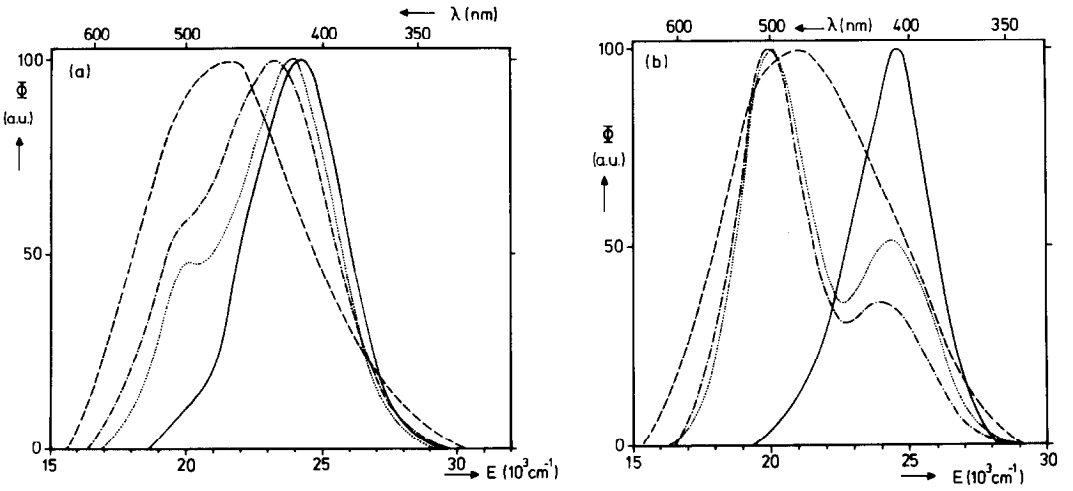

FIG. 4. Emission spectrum of $Y(PO_3)_3$–Sb^{3+} for λ_{exc} = 245 nm (a) at T = 6 K (—), 70 K (···), 140 K (-·-·-), and 270 K (---) and for λ_{exc} = 260 nm (b) at T = 6 K (—), 55 K (···), 70 K (-·-·-), and 260 K (---). All spectra are normalized.

nm (40,000 cm^{-1}) and 235 nm (42,500 cm^{-1}). At higher temperatures (20 K < T < 150 K) the lower energy part of the excitation band vanishes and the excitation maximum is at about 235 nm. For temperatures above 150 K the broad excitation band reappears.

For emission wavelength 500 nm, the excitation band between 20 and 150 K consists of a doublet with maxima at about 255 nm (39,200 cm^{-1}) and 235 nm (42,500 cm^{-1}). At higher temperatures the excitation consists of a broad band with its maximum between 235 and 250 nm. For emission wavelength 450 nm (T > 150 K) the same broad excitation band is found.

As for $Ln(PO_3)_3$–Sb^{3+} (Ln = Sc, Lu, Gd) the excitation bands are ascribed to the $^1S_0 \rightarrow {}^3P_1$ transition and the emission bands to the $^3P_{1,0} \rightarrow {}^1S_0$ transition. The observed emission and excitation spectra will be superpositions of the emission and excitation bands of the different Sb^{3+} centers in $Y(PO_3)_3$–Sb^{3+}. They are independent of the Sb concentration and of sample preparation (see Section 2.1). Therefore, the occurrence of several emission bands cannot be

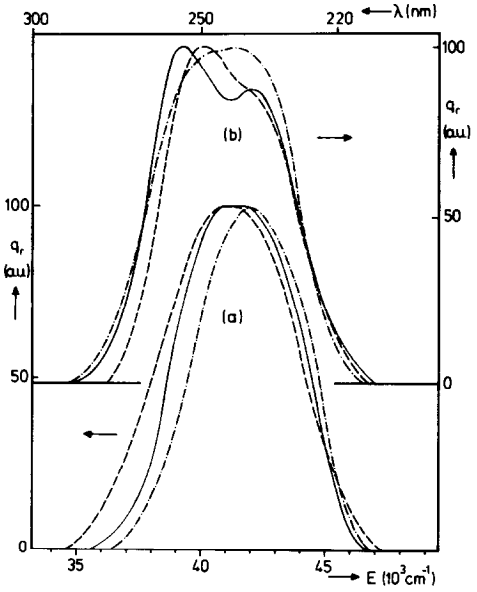

FIG. 5. Excitation spectrum of the emission of $Y(PO_3)_3$–Sb^{3+} for λ_{em} = 400 nm (a) at T = 5.5 K (—), 60 K (-·-·-), and 200 K (---) and for λ_{em} = 500 nm (b) at T = 43 K (---), 78 K (—), 160 K (-·-·-). All spectra are normalized. The emission wavelengths are selected using a cut-off filter (λ_{em} > 360 nm) and band-pass filters (380 < λ_{em} < 420 nm (a); 480 < λ_{em} < 520 nm (b)).

ascribed to clusters or pairs of Sb^{3+} ions or to energy transfer from one center to another (there is no overlap between the emission and excitation bands).

The only satisfactory way to explain the observed spectra is to assume that the Jahn–Teller effect is acting on the relaxed excited state (RES) of some of the Sb^{3+} centers. The Jahn–Teller effect has often been observed for mono- and divalent s^2 ions in alkali halides (*1, 23*), as well as for Sb^{3+} in $LnPO_4$ (*Ln* = Sc, Lu, Y) (*5, 6*), and may lead to two different minima on the adiabatic potential energy surface (APES) of the ^3P RES. These minima arise from the interaction of the orbital triplet state with local vibrational modes and give rise to two emission bands, the intensity ratio of which is strongly temperature dependent. It is well known that the occurrence of two kinds of minima on the APES of the ^3P RES depends critically on the balance between several factors, among others the spin-orbit coupling and electron-lattice interaction (*1, 15, 23*). Small changes in some of these factors might be the reason that for $Ln(PO_3)_3$–Sb^{3+} (*Ln* = Sc, Lu, Gd) only one kind of minimum occurs. In addition, it should be taken into account that small changes in the emission from one or two sites will be obscured by overlap with the emission from the other sites.

The coordination of Sb^{3+} at the different sites in $Y(PO_3)_3$ can be compared to that of monovalent s^2 ions in alkali halides in which the s^2 ion is octahedrally coordinated by the halide ions. All four sites in $Y(PO_3)_3$ provide a six coordination by oxygen ions. Two of these sites possess inversion symmetry and are actually rather close to O_h symmetry. This makes it plausible that the ^3P levels of Sb^{3+} ions at these sites are distorted by the Jahn–Teller effect.

From Fig. 4b it is clear that the Sb^{3+} centers for which the Jahn–Teller effect (JTE) is observed show two emission bands with maxima at about 415 nm (24,000 cm^{-1}) and 500 nm (20,000 cm^{-1}). At 6 K only the 415-nm emission is observed. At higher temperatures ($T > 20$ K) the other minimum becomes thermally populated leading to emission at 500 nm. The same features are observed in Fig. 4a, although less clearly than in Fig. 4b. Apparently, these double-minimum JT-active Sb^{3+} centers are more efficiently excited in the lower energy part of the excitation spectrum. The emission of the Sb^{3+} centers for which the JTE does not lead to two minima on the APES of the ^3P RES, consists of only one band with its maximum at about 415 nm. This band overlaps with the higher energy emission band of the double-minimum JT-active centers.

Unfortunately, it is not possible to distinguish between the excitation spectra of the double-minimum and single-minimum Sb^{3+} centers at 6 K. However, for the temperature region in which the 500-nm emission band has a high intensity, the excitation spectra of these centers can be distinguished to some extent (compare Figs. 5a and 5b for 20 K $< T <$ 100 K). Figure 5b shows that the $^1S_0 \rightarrow {}^3P_1$ excitation band of the double-minimum centers consists of a doublet. This doublet structure must be found for s^2 ions on which the Jahn–Teller effect is working (*24, 25*) and supports our assumption that the occurrence of several emission bands must be ascribed to the JTE.

The maxima of the emission bands of s^2 ions with a double minimum in the RES shift with temperature due to the asymmetry of these minima (*6, 23*). This leads for high temperatures ($T > 160$ K) to the observation of one broad emission band, which is a superposition of the emission bands of all Sb^{3+} centra (Fig. 4).

It is interesting to note that for the double-minimum Sb^{3+} centers the extra emission band is found at 500 nm, since the position of the emission band at 415 nm corresponds to the positions of the single-minimum emission bands of $Ln(PO_3)_3$–Sb^{3+}

(*Ln* = Sc, Lu, Gd). According to Fukuda (*23*), the higher energy emission band can be ascribed to A_T emission and the lower energy emission band to A_X emission. This is in agreement with monovalent s^2 ions in rocksalt-structured alkali halides. For *Ln* PO_4–Sb^{3+} (*Ln* = Sc, Lu, Y), in which Sb^{3+} is eightfold coordinated by oxygen atoms, this situation is reversed (*6*) in agreement with CsBr–In^+ and CsI–In^+ in which the s^2 ion is also eightfold coordinated (*26*).

Decay time measurements. Only decay times of the 415-nm emission band could be measured. The 500-nm emission band appears at temperatures above 20 K, where the decay times are already too short to be measured. In comparison with *Ln*$(PO_3)_3$–Sb^{3+} (*Ln* = Sc, Lu, Gd) the decay curves showed an intermediate behavior: neither the one-exponential nor the two-exponential fitting results were completely satisfactory. This is in line with the radius of the Y^{3+} ion, viz. 0.900 Å (*13*), which is in between that of Lu^{3+} and Gd^{3+} (see section 3.1 and Table II). The decay times obtained by both the one-exponential and two-exponential fitting procedures were fitted to a three-level scheme (*19, 20*). The results are given in Table III.

3.3 La$(PO_3)_3$–Sb^{3+}

The La$(PO_3)_3$–Sb^{3+} samples showed a bluish luminescence under UV excitation with a quantum efficiency of only some 10% at 300 K. In this composition only one site is available for the Sb^{3+} ion. As a consequence the emission and excitation bands are narrower than in the case of *Ln*$(PO_3)_3$–Sb^{3+} (*Ln* = Sc, Lu, Y, Gd) as mentioned in Section 3.1.

The emission consists of one band with its maximum at 455 nm (22,000 cm^{-1}). The maximum of the excitation band is found at 240 nm (41,500 cm^{-1}). Temperature quenching is observed for temperatures above 240 K. A weak emission around 330 nm is ascribed to Ce^{3+} which is a common impurity in the starting compound La_2O_3.

The emission band is assigned to the $^3P_1 \rightarrow {}^1S_0$ transition (or the $^3P_0 \rightarrow {}^1S_0$ transition at low temperatures), while the excitation band is assigned to the $^1S_0 \rightarrow {}^3P_1$ transition. The Stokes shift amounts to 19,500 cm^{-1}. This large Stokes shift can be explained by the large space available for the Sb^{3+} ion (*18*). Comparable Stokes shifts are observed for $LaBO_3$–Sb^{3+} (*4*) and for Sb^{3+} in calciumhalophosphate (*12*).

The decay curves of the 455-nm emission band were clearly one-exponential, reflecting that only one Sb^{3+} center is present. The decay times could well be fitted to a three-level scheme yielding a $^3P_0 \rightarrow {}^1S_0$ decay time (τ_0) of 690 ± 10 μs, a $^3P_1 \rightarrow {}^1S_0$ decay time (τ_1) of 1.6 ± 0.3 μs, and an energy difference between the $^3P_1$ and $^3P_0$ levels (ΔE) of 30 ± 1 cm^{-1}. This small ΔE value is in line with the large Stokes shift.

Acknowledgment

The authors are indebted to Mr. G. J. Dirksen for performing the atomic absorption measurements.

References

1. A. Ranfagni, D. Mugnai, M. Bacci, G. Viliani, and M. P. Fontana, *Adv. Phys.* **32,** 823 (1983).
2. G. Blasse, *Rev. Inorg. Chem.* **5,** 319 (1983).
3. A. Wolfert, E. W. J. L. Oomen, and G. Blasse, *J. Solid State Chem.* **59,** 280 (1985).
4. E. W. J. L. Oomen, L. C. G. van Gorkom, W. M. A. Smit, and G. Blasse, *J. Solid State Chem.* **65,** 156 (1986).
5. E. W. J. L. Oomen, W. M. A. Smit, and G. Blasse, *Chem. Phys. Lett.* **112,** 547 (1984).
6. E. W. J. L. Oomen, W. M. A. Smit, and G. Blasse, *Phys. Rev. B* **37** (1988).
7. P. P. Melnikov, P. H. Komussarova, and T. A. Lymysova, *Izv. Akad. Nauk. SSSR, Neorg. Mater.* **17,** 2110 (1981).
8. H. Y. P. Hong, *Acta Crystallogr. Sect. B* **30,** 468 (1974).
9. M. Bagieu-Beucher, *J. Appl. Crystallogr.* **9,** 368 (1976).

10. H. Y. P. HONG, *Acta Crystallogr. Sect B* **30,** 1857 (1974).
11. R. C. M. PEETERS, unpublished results; M. BUYS, unpublished results.
12. G. BLASSE, *Chem. Phys. Lett.* **104,** 160 (1984).
13. R. D. SHANNON AND C. T. PREWITT, *Acta Crystallogr. Sect. B* **25,** 925 (1969).
14. E. W. J. L. OOMEN, W. M. A. SMIT, AND G. BLASSE, *J. Phys. C* **19,** 3263 (1986).
15. E. W. J. L. OOMEN, G. J. DIRKSEN, W. M. A. SMIT, AND G. BLASSE, *J. Phys. C* **20,** 1161 (1987).
16. A. C. VAN DER STEEN, J. J. P. VAN HESTEREN, AND A. P. SLOK, *J. Electrochem. Soc.* **128,** 1327 (1981).
17. C. W. M. TIMMERMANS AND G. BLASSE, *J. Solid State Chem.* **52,** 222 (1984).
18. W. M. A. SMIT AND E. W. J. L. OOMEN, *in* "Fall Meeting of the Electrochemical Society, San Diego, 1986," Extended abstracts, Vol. 86-2, No. 699.
19. A. E. HUGHES AND G. P. PELLS, *Phys. Status Solidi B* **71,** 707 (1975).
20. G. BOULON, C. PEDRINI, M. GUIDONI, AND CH. PANNEL, *J. Phys.* **36,** 267 (1975).
21. G. BLASSE AND A. C. VAN DER STEEN, *Solid State Commun.* **31,** 993 (1979).
22. D. MUGNAI, A. RANFAGNI, O. PILLA, G. VILIANI, AND M. MONTAGNA, *Solid State Commun.* **35,** 975 (1980).
23. A. FUKUDA, *Phys. Rev. B* **1,** 4161 (1970).
24. A. FUKUDA, *Sci. Light (Tokyo)* **13,** 64 (1964).
25. Y. TOYOZAWA AND M. INOUE, *J. Phys. Soc. Japan* **21,** 1663 (1966).
26. D. J. SIMKIN, T. F. BELLIVEAU, V. S. SIVASANKAR, K. SCHMITT, AND P. W. M. JACOBS, *J. Luminescence* **31, 32,** 320 (1984).